2019 2nd IEEE International Conference on Soft Robotics (RoboSoft)
COEX, Seoul, Korea, April 14-18, 2019

Development of a Vision-Based Soft Tactile Muscularis

Lac Van Duong, Rei Asahina, Jia Wang, and Van Anh Ho

Abstract— **In this paper, we introduce our preliminary results in the development of a vision-based tactile sensing system at large scale, called muscularis. The muscularis is an elongated structure with a rigid transparent bone covered by a soft tactile skin whose stiffness can be varied by pressurization of a chamber. Inner layer of the skin is covered by an array of markers with reflective white coating paint. Two cameras are layout at two ends of the muscularis for tracking three-dimensional movement of markers under interaction with surrounding environment (including humans). We also proposed a method for real-time construction of the muscularis's tactile information under physical interaction/impact. As a result, the muscularis can estimate detailed movements of all markers, and interpret information of multiple contact locations. The developed tactile muscularis can be integrated on the standard articulate robotic arm for enhancement of the robot's interaction with the surroundings under physical acting. This work is also expected to pave a way for the development of a friendly robot with proper tactile sensing for safe and comfortable interaction with humans.**

I. Introduction

Nowadays, with the development of robotics, soft robots tend to be softened with the high awareness of interaction with the surroundings. Especially, soft haptic interfaces, which can assess tactile information from physical interaction through soft media, are of promising research toward safe and informative interfaces for the promotion of human-robot interaction. With such sensor interfaces, robots can not only avoid hurting human unintentionally, but also sense the physical interaction and respond safely and friendly with the human.

A. Tactile sensing system

In order to sense robots' physical interaction with surrounding environment, there were numerous research reported on the development of tactile sensing systems that can detect multimodalities of touch, mostly for robotic fingers/hands [1]. These sensors were commonly designed in multi-sensing elements with operating principle based on transducing from applied stress/strain to the change of resistance [2], capacitance [3], inductance [4], electromagnetics [5], and so on. However, these devices met the difficulty in fabrication and function at a larger scale and higher resolution, since an increasing number of sensing elements and reduce the size of the electronic acquisition systems are challenging issues.

Duong, Asahina, Wang and Ho are with School of Materials Science, Japan Advanced Institute of Science and Technology (JAIST), 1-1 Asahidai, Nomi, Ishikawa, Japan. Email:{lacduong, s1710005, s1810028, van-ho}@jaist.ac.jp

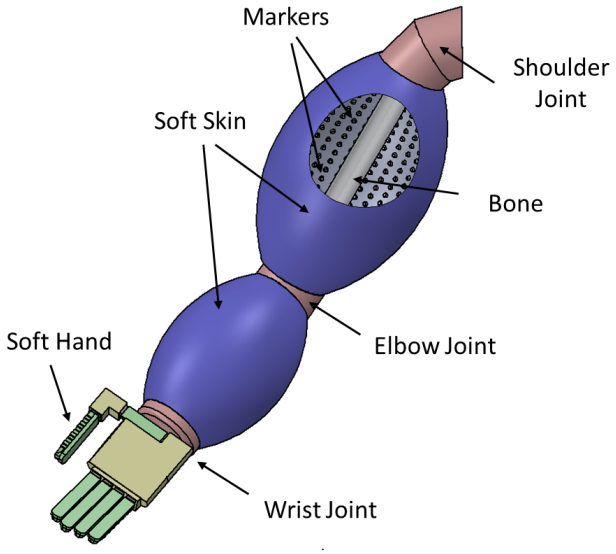

Fig. 1. The ultimate design of a soft interactive robot arm with high tactile resolution, variable stiffness and controllable shape.

B. Vision-based tactile sensing systems

Vision-based tactile technology may help overcome such issues, since with current technology in hardware cameras are miniaturized with high resolution. In this technique, the camera is used to track a large number of markers/dots which move under applied load. Ho *et al* [6] proposed a method of using tactile image to the task of sliding detection. However, this method is only applicable in static condition. The design reported in [7] estimated the external force by solving the equilibrium equations in each compartmentalized segment of the membrane and dealt with real-time performance. Yuji Ito *et al*. proposed the contact region estimation based on a vision [8], where they formulated an equation to discriminate between the contacting dots and the non-contacting dots; nonetheless, this method was found complicated to be applied in multi-point contacting and in large scale. TacTip family is a typical design of vision-based tactile sensing system for small-scale applications (robotic fingertip, hand), and has been reported with promising functions in slip detection [9], tactile exploration [10], object manipulation [11]. Nonetheless, extracted information from TacTip is two-dimensional (2-D) displacement of markers, while markers actually move in 3-D space. GelSight is another example on the utilization of camera may lead to a very informative tactile sensing system [12], although the scalability of this sensing system has not been reported.

978-1-5386-9260-8/19/$31.00 ©2019 IEEE

C. Large scale tactile sensing system

Recently, many researches attempted to cover the entire robot with tactile skin for the enhancement robot's awareness in interaction with the surroundings. HEX-O-SKIN [13] is a tiled robotic skin from the hexagonal circuit integrated with many types of sensing elements. This design can bring diverse perception of robot. However, it is not soft, and fabrication and data acquisition are rather expensive. Alexander *et al*. [14] developed a soft arm covered by an inflatable outer skin with one pressure sensor. This design, however, cannot determine the contact location. A. Stilli in [15] proposed an articulated robot arm with pneumatic variable stiffness links. This design also only detected collision through reading pressure inside the link. As a similar approach, Kim *et al*. [16] developed a sensing module is made from elastomer skin with an embedded EGaIn-based tactile sensor. By measurement of variable resistance, deformation on the skin can be estimated, resulting in the perception of collision and a light touch of the robot arm with the human. However, the resolution is coarse for the detection of diverse interaction from the human.

D. Contribution of this research

In order to equip the entire robot with tactile skin for assessment of human's diverse interaction, we constructed a hybrid design with rigid, transparent bone and soft skin, mimicking the anatomy of human's arms (Fig. 1). This work is expected to contribute to the field of soft haptic interaction with a feasible design for human-robot interaction in a large scale. In this paper, we present the detailed design and fabrication process of the muscularis in section II, followed by a vision-based system model in section III. We then show some preliminary results in the evaluation of the sensing ability of the proposed model in section IV. Finally, in section V we point out the current issue and plan for this research.

II. Design and Fabrication

A. Muscularis Design

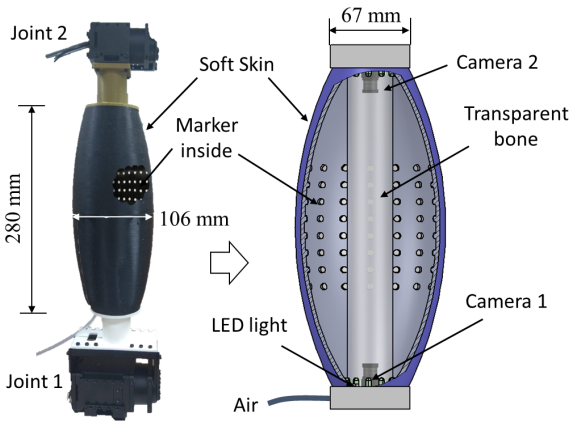

Fig. 2. Soft muscularis with inner markers and two co-axial cameras located at two ends. Each marker is coated with the reflective paint, and the white LEDs source was distributed around each camera.

The motivation for the proposal of the muscularis is to create tactile sensing modules that can be integrated into robotic arms as links connecting joints. Notably, the vision-based technique was chosen for the accomplishment of high tactile resolution without complicated wiring as in common embedded tactile sensing systems. The detailed design of the muscularis is illustrated in Fig. 2. An elongated hollow 3D model with tapering ends (corn-shaped) is made by the silicone rubber. Compressed air can be applied to the muscularis' inner space for changing the shape and the stiffness. The shape and size of the muscularis were designed considering the anatomy of humans' arm. On the inner wall of the muscularis, there are multiple fiducial dots (markers) distributed regularly. This design is inspired by the work of Ito [7] and TacTip [9]. While markers of TacTip family was tracked by one camera with two-dimensional output on a smaller scale (finger), we aim to track 3D movement of trackers by the stereo camera. This includes two cameras located at two ends of the muscularis. Each marker (or dot) emerges 3mm from the inner wall, with diameter of 2mm, and resolution is 15mm. This distribution is not fixed and only proposed for preliminary evaluation in this paper. In order to completely eliminate the effect of surrounding light, the muscularis is set to be black, and markers are white. A thin transparent and stiff and pipe rod is set up to connect two ends of the muscularis for maintain the strength of the robotic arm.

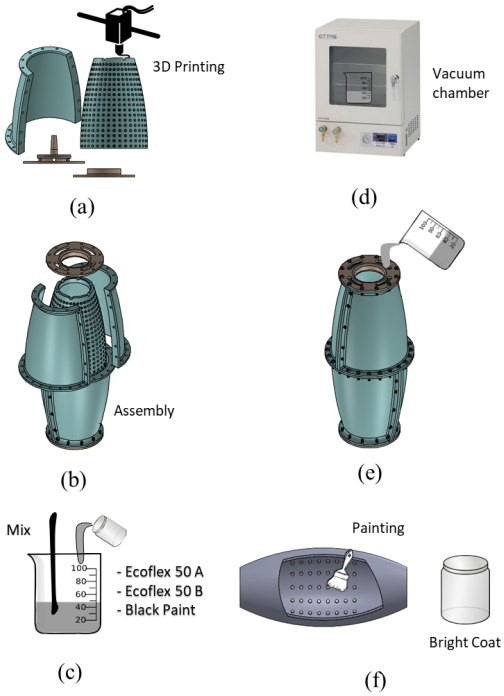

Fig. 3. Fabrication process: (a) Molding printing, (b) Mold assembling, (c) Mixing the silicon rubber with black paint, (d) Getting rid of bubbles, (e) Casting, (f) Coating inner dots with reflective paint.

B. Fabrication

Fig. 3 illustrates the main parts of the molding/casting process using silicon rubber for muscularis' skin.

a) First, a 3D printer (M200, Zortrax) is utilized to print eight separate parts of the molds, considering the maximum printable space of the printer.
b) After printing, we use screws/nuts to assemble the parts. In order to avoid uncured silicone from leaking out during casting, we seal boundaries with a thin layer of silicon rubber.
c) Then, we mix the silicon liquid by part A, part B of off-the-shelf silicone rubber (EcoFlex 00-50, Smooth-On, USA), and black silicone pigment (Silc Pig, Smooth-On) in the measuring glass.
d) The mixed silicon will be degassed in the vacuum chamber about 5 minutes.
e) Pour the mixture into the mold. The silicon is completely cured in the room temperature at about 5 hours to form a competed muscularis' skin with dots distributed in the inner wall.
f) A reflective paint (Bright coat N, Komatsu Process Lmtd., Japan) is used to coat the dot of makers to increase the reflectivity of the markers.

III. Vision-Based System

A. Camera model

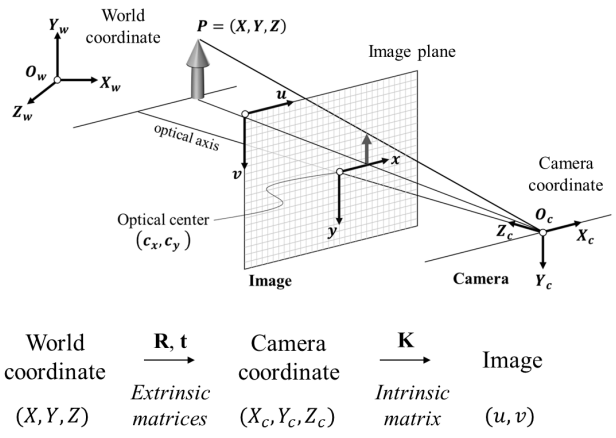

Fig. 4. The pinhole camera model. [17]

In this research, we use the camera based on the pinhole model and its parameters mentioned in [18]. The pinhole camera model (Fig. 4) is based on the principle of collinearity, where each point P is projected by a straight line through the principle point into the image plane. The relation between the real 3D point in world coordinate $\mathbf{X} = (X, Y, Z, 1)^T$ and its projection in the image plane $\mathbf{u} = (u, v, 1)^T$ is given by

$$\mathbf{u} = \mathbf{P} \times \mathbf{X}, \tag{1}$$

where $\mathbf{P}$ is 3×4 projection matrix.

The extrinsic parameters define the location and orientation of the world coordinate expressed in the camera coordinate system by the rotation matrix $\mathbf{R}$ the and translation vector $\mathbf{t}$. The camera intrinsic matrix $\mathbf{K}$ only depends on the characteristic of the camera sensor and lens as

$$\mathbf{K} = \begin{bmatrix} f_x & s & c_x \\ 0 & f_y & c_y \\ 0 & 0 & 1 \end{bmatrix}, \tag{2}$$

where f_x, f_y are the focal length, (c_x, c_y) is the optical center point in pixels, s is skew coefficient which is non-zero if the image axes are not perpendicular.

From the camera parameters, the projection matrix can be obtained as

$$\mathbf{P} = \mathbf{K}\left[\mathbf{R}|\mathbf{t}\right]. \tag{3}$$

The camera matrix (Eq. 3) does not account for lens distortion. To increase accuracy, the camera model should include the radial and tangential lens distortion parameters. In this paper, we only considered the radial distortion with the distorted point is defined [19]

$$\begin{aligned} x_{corrected} &= x(1 + k_1 r^2 + k_2 r^4 + k_3 r^6) \\ y_{corrected} &= y(1 + k_1 r^2 + k_2 r^4 + k_3 r^6) \end{aligned}, \tag{4}$$

where $x = u - c_x$, $y = v - c_y$; k_1, k_2, k_3 are the distortion coefficients and $r^2 = x^2 + y^2$.

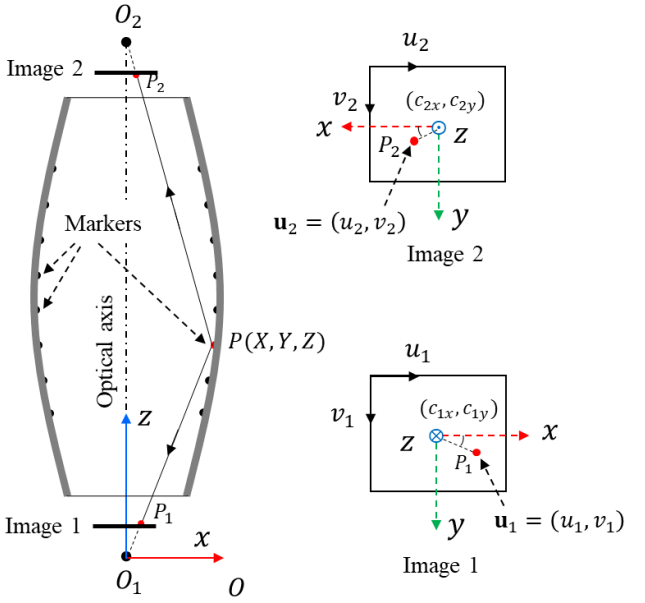

Fig. 5. The configuration of the stereo cameras system. The two cameras are installed along the muscularis at two ends

We suppose that a point/marker $P(X, Y, Z)$ is visible onto two cameras (Fig. 5). From two views we have $\mathbf{u}_1 = \mathbf{P}_1\mathbf{X}$ and $\mathbf{u}_2 = \mathbf{P}_2\mathbf{X}$ corresponding to known projection P_1 and P_2 in two images with four linear equations of $\mathbf{X}$, which is written in the form of $\mathbf{AX} = \mathbf{b}$. Thus, the triangulation problem is to find the point $P(X, Y, Z)$ which can be given by solving the least-squares minimization problem as following

$$\|\mathbf{AX} - \mathbf{b}\|^2 = \sum_{i=1}^{4} (\mathbf{A}_i\mathbf{X} - \mathbf{b}_i)^2 \to 0. \tag{5}$$

where $\mathbf{A}_i$ is the i-th row of matrix $\mathbf{A}$.

B. Camera calibration

To obtain the stereo camera parameters, we use a checkerboard pattern as one standard procedure to calibrate the cameras. The checkerboard should contain an even number of squares one side and the other side contains an odd number of squares that support to determine the orientation of the pattern. The calibration procedure was implemented in Matlab® [20]. By taking a planar checkerboard with known dimensions in different views with two cameras, the projection matrices of the cameras were obtained. Results of intrinsic parameters were presented in Table I.

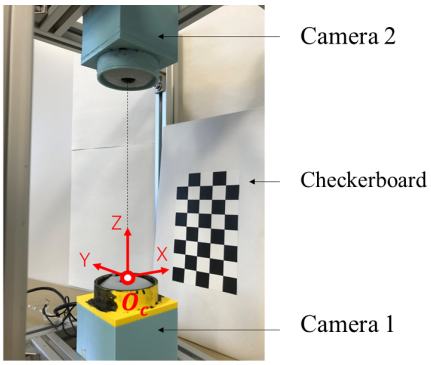

Fig. 6. Calibration setup, the pattern of 5×8 squares with the size of each square is $20 \times 20\,\text{mm}^2$. The distance between the two cameras is 280 mm

TABLE I
INTRINSIC CAMERA PARAMETERS*

Parameter	f_x	f_y	c_x	c_y
Camera 1	264.4	254.7	332.8	221.1
Camera 2	262.5	251.3	316.0	240.4

*All values are unit in pixels.

C. 3D tactile reconstruction

In order to sense the external force, it is possible to track the markers' position to determine the muscularis deformation and the acting force applied to it. The following five steps to determine the tactile information.

1) The captured pictures from cameras are undistorted to compensate for the radial distortion of lens and then converted into gray scale image. as shown in Fig. 7(a)
2) Images are preprocessed to enhance the contrast of markers in the gray space.
3) The regions of the markers are extracted by using threshold to binarize the images finding the centroids of markers.
4) Markers are identified by frame-by-frame in which the position of each marker is tracking base on the previous time. The corresponding markers on two cameras are numbered and matched as illustrated in Fig. 7(b)
5) Compute the triangulation problem (Eq. 5) and the three-dimensional tactile information is constructed as shown in Fig. 7(c)

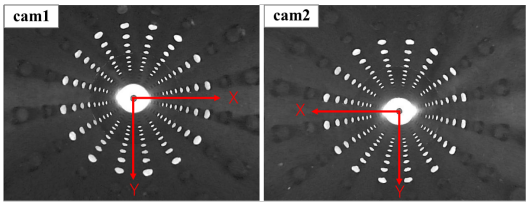

(a) The undistorted images

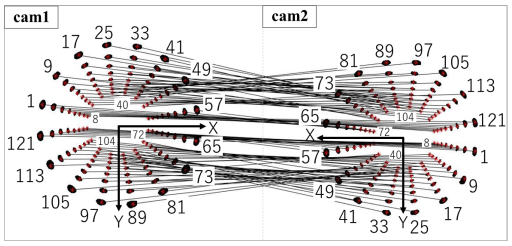

(b) Markers tracking and matching

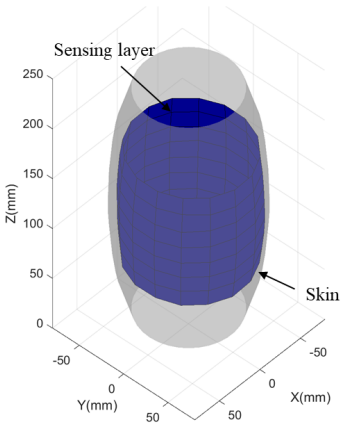

(c) The 3D tactile information

Fig. 7. The image processing for tactile reconstruction.

IV. EXPERIMENT AND EVALUATION

A. Experiment setup

In this experiment, we evaluate the performance of deformation sensing by setting up a testbed for data acquisition and conducting several preliminary experiments on human physical interaction. The experiment setup is shown in Fig. 8. The muscularis' two ends are mounted onto two camera boxes which are attached on a frame. Each camera box has one miniaturized CMOS cameras, resolution of 640×480 pixels with a fisheye lens. The compressed air is supplied by a compressor (JUNAir) through a pressure regulator (SMC ITV2030-212BS). A program was written on MATLAB implements the data acquisition and real-time tracking process. The program runs on ordinary PC with Window 10, the speed of the processor used in the PC is Intel Core i5-7200U 2.5GHz. The sampling and computation processes are performed with a frequency of 16Hz and 8Hz.

We then conducted physical interaction for evaluation of the muscularis's deformation sensing at a specific value of compressed air. First, the pressure of the inner chamber was

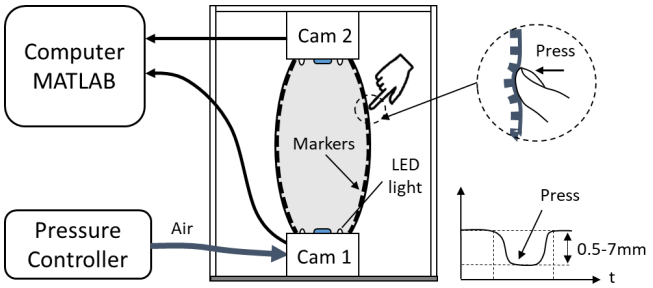

Fig. 8. The experiment set up. The muscularis is mounted on a box. LEDs illuminate markers and two fisheye cameras track their displacement. "Note that, in this preliminary evaluation the transparent bone was not included"

maintained at 2 kPa by the SMC pressure regulator in order to provide the muscularis skin with a proper stiffness and shape. Then, simple physical interactions by fingers were applied at different locations at the same time with the amplitude of deformation from 0.5-7 mm (Fig. 8). The program calculated the three movements (x, y, and z) of all makers over time, and render the 3D tactile information in the real-time. The time cost for each loop is approximately 0.13 sec.

B. Results and evaluation

In this test, we implemented the interaction at two different locations, in which the applied forces are perpendicular to the surface around point 40 and point 83 at the same time. Fig. 9 illustrates the 3D tactile information and Fig. 10 is the estimated displacement results (in mm) of all the markers (128 points) during interaction with detailed and intuitive deformation of the muscularis' skin in real-time.

Specifically, Fig. 10(a) is the displacement in the x-axis with the amplitude in the range of 0-2.73 mm, the maximum impact point in the positive direction of x-axis is point 83 with a magnitude of 2.73 mm, and point 43 is the most displaced in the negative direction of x-axis with a magnitude of 2.15 mm.

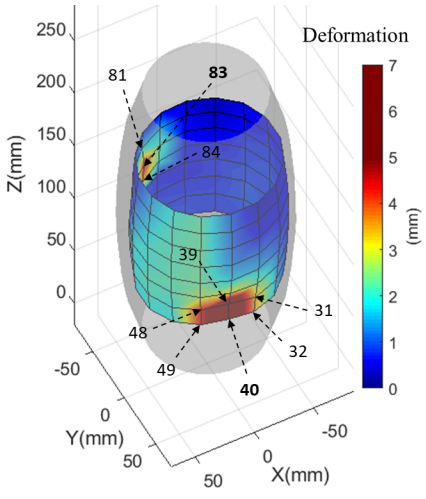

Fig. 9. Real-time reconstruction of 3-dimensional tactile information under physical contacts, mainly at point 40 and 83.

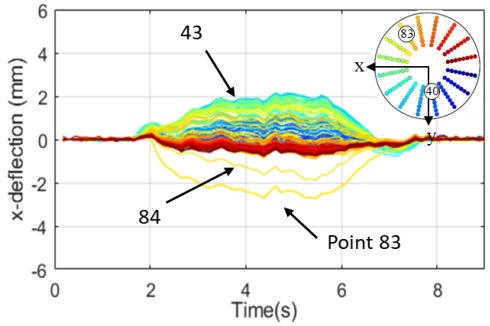

(a) The x-axis deflection

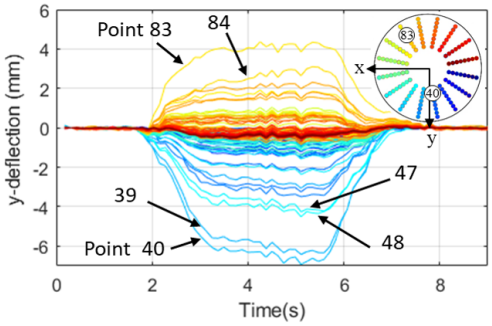

(b) The y-axis deflection

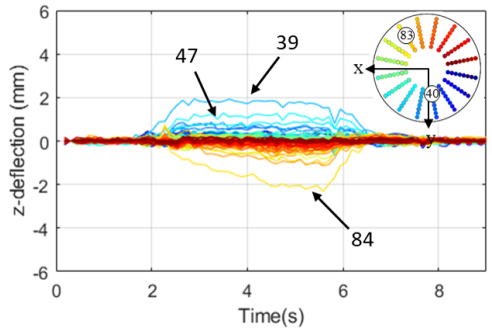

(c) The z-axis deflection

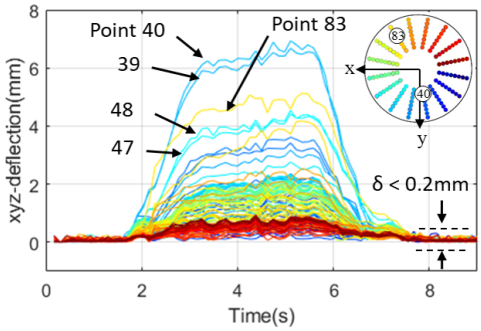

(d) The absolute deflection

Fig. 10. The estimated deflection for each marker, localization/number of markers corresponds to the color in Fig. 11; (a) maker deflection along the x-axis, (b) along the y-axis, (c) along the z-axis, (d) total deflection in three directions.

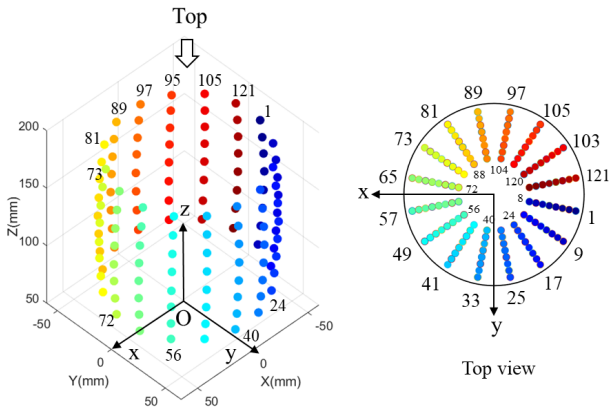

Fig. 11. Location and numbering of markers with corresponding colors: entire view (left) and top view (right).

Similarly, the most significant impact on the y-axis is points 83 with an amplitude of 4.36 mm, the largest on the negative direction of the y-axis is point 40 with an amplitude of 6.93 mm (Fig. 10(b)). For z-axis, the greatest impact on the z-axis is point 39 with the amplitude of 1.94 mm, and the largest on the negative y-axis is point 84 with the amplitude of 2.32 mm (Fig. 10(c)).

Fig. 10(d) is the absolute displacement of the points in 3D space. By using the soft tactile muscularis, it is possible to assess the location of contact and magnitude of displacement on the skin due to physical contact. Consequently, according to the above preliminary results, we confirmed the muscularis' ability in the localization of the multiple contact and determination of skin's deformation during interaction with the surrounding environment based on detailed tracking of markers using the stereo camera. Note that the above results are obtained in one specific condition of the inner pressure, *i.e.* stiffness of the skin. Since the stiffness is variable, it is expected that the sensitivity of the muscularis can be changed accordingly.

V. Conclusion and Future Work

In this paper, in order to develop a whole-body soft tactile robot for the promotion of human-robot interaction, we presented an idea, design, fabrication process, calibration and preliminary experimental results of a soft tactile muscularis that has scalable structure, high resolution, and variable stiffness. Initial results show the feasibility of the proposed design in obtaining a detailed 3D displacement of inner markers using two cameras, resulting in the assessment of tactile information of the muscularis skin during interaction. This design is expected to be scalable, not only in size but also in resolution and stability; thus, it can act as a platform for providing rich information of touch to improve the interaction with humans.

In the next work, we will build the Finite Element Model describing the relationship of the external force (including the pressurized force) and deformation. As result, the acting force can be calculated through the camera's information. The performance of the system will be enhanced by optimizing the image processing algorithm or implemented on the high-speed hardware platform such as field-programmable gate array (FPGA). Strikingly, the muscularis will be intelligent by using deep learning for interpreting human's tactile primitives and its related emotional factor. Base on this approach, we desire to develop a new generation of robotic application that the robot will complete understanding and sensing the humans' diverse interaction.

References

[1] Ravinder S. Dahiya, Giorgio Metta, Maurizio Valle, Giulio Sandini, "Tactile Sensing-From Humans to Humanoids", *IEEE Transactions on Robotics*, Vol. 26, No. 1, February 2010.

[2] H. Zhang and E. So, "Hybrid resitive tactile sensing", *IEEE Trans. Syst*, Man, Cybern. B, Vol. 32, No. 1, pp. 57–65, Feb. 2002.

[3] K. Suzuki, K. Najfi, and K.D. Wise, "A1024-element high-performance silicon tactile imager", *in Proc. IEEE Elect. Devices Meeting*, pp. 674–677, 1988.

[4] Hongbo Wang, Gregory de Boer, Lucia Beccai, Ali Alazmani, Peter Culmer, "Design and Characterization of Tri-Axis Soft Inductive Tactile Sensors", *IEEE Sensors Journal*, No. 19, Oct 2018.

[5] S. Wattanasarn, K. Noda, K. Matsumoto, I. Shimoyama, "3D flexible tactile sensor using electromagnetic induction coils", *2012 IEEE 25th International Conference on Micro Electro Mechanical Systems*, 29 Jan.-2 Feb. 2012

[6] Van Anh Ho, T. Nagatani, A. Noda, and Shinichi Hirai, What Can Be Inferred From a Tactile Arrayed Sensor in Autonomous In-Hand Manipulation?, *2012 IEEE Int. Conf. on Automation Science and Engineering(CASE)*, pp.457-464, Seoul, Korea, Aug. 20-24, 2012.

[7] Yuji Ito, Youngwoo Kim, Goro Obinata, "Multi-axis force measurement based on vision-based fluid-type hemispherical tactile sensor", *2013 IEEE/RSJ International Conference on Intelligent Robots and Systems*, DOI:10.1109/IROS.2013.6697037

[8] Yuji Ito, Youngwoo Kim, Goro Obinata, "Contact Region Estimation Based on a Vision-Based Tactile Sensor Using a Deformable Touchpad", *Sensors (Basel)*, 2014 Apr; 14(4): 5805–5822.

[9] Jasper Wollaston James, Nicholas Pestell, Nathan F. Lepora, "Slip Detection With a Biomimetic Tactile Sensor", *IEEE Robotics and Automation Letters*, Vol. 3, Issue: 4, Oct. 2018.

[10] Nicholas Pestell, John Lloyd, Jonathan Rossiter, Nathan F. Lepora, "Dual-Modal Tactile Perception and Exploration", *IEEE Robotics and Automation Letters*, Vol. 3, Issue: 2, April 2018.

[11] B. Ward-Cherrier et al, "The TacTip Family: Soft Optical Tactile sensors with 3D-Printed Biomimetic Morphologies", *Soft Robotics*, Vol. 5, No 2, April, 2018.

[12] Wenzhen Yuan, Siyuan Dong, and Edward H. Adelson, "MGelSight: High-Resolution Robot Tactile Sensors for Estimating Geometry and Force", *Sensors*, 2017, 17(12), 2762.

[13] Philipp Mittendorfer, Gordon Cheng, "Humanoid Multimodal Tactile-Sensing Modules", *IEEE Transactions on Robotics*, Vol: 27, Issue: 3, June 2011.

[14] Alexander Alspach, Joohyung Kim, and Katsu Yamane, "Design and Fabrication of a Soft Robotic Hand and Arm System", *IEEE-RAS International Conference on Soft Robotics 2018*, April 25, 2018.

[15] Agostino Stilli, Luca Grattarola, Hauke Feldmann, "Helge A. Wurdemann, Kaspar Althoefer, Variable Stiffness Link (VSL): Toward inherently safe robotic manipulators", *2017 IEEE International Conference on Robotics and Automation (ICRA)*, 29 May-3 June 2017.

[16] Katsunari Sato, Kazuto Kamiyama, Hideaki Nii, Naoki Kawakami, Susumu Tachi, "Measurement of force vector field of robotic finger using vision-based haptic sensor", *2008 IEEE/RSJ International Conference on Intelligent Robots and Systems*, 22-26 Sept. 2008.

[17] MATLAB, "What is Camera Calibration?", *The MathWorks*, Retrieved from https://www.mathworks.com/help/vision/ug/camera-calibration.html, 2018.

[18] Richard Hartley, "Multiple View Geometry in Computer Vision, Second Edition", *Cambridge University Press*, 2004.

[19] Brown, Duane C, "Decentering distortion of lenses", *Photogrammetric Engineering*, 32 (3): 444–462, May 1966

[20] MATLAB 2018b, "Stereo Camera Calibrator App", *The MathWorks*, Inc., Natick, Massachusetts, United States 2018.